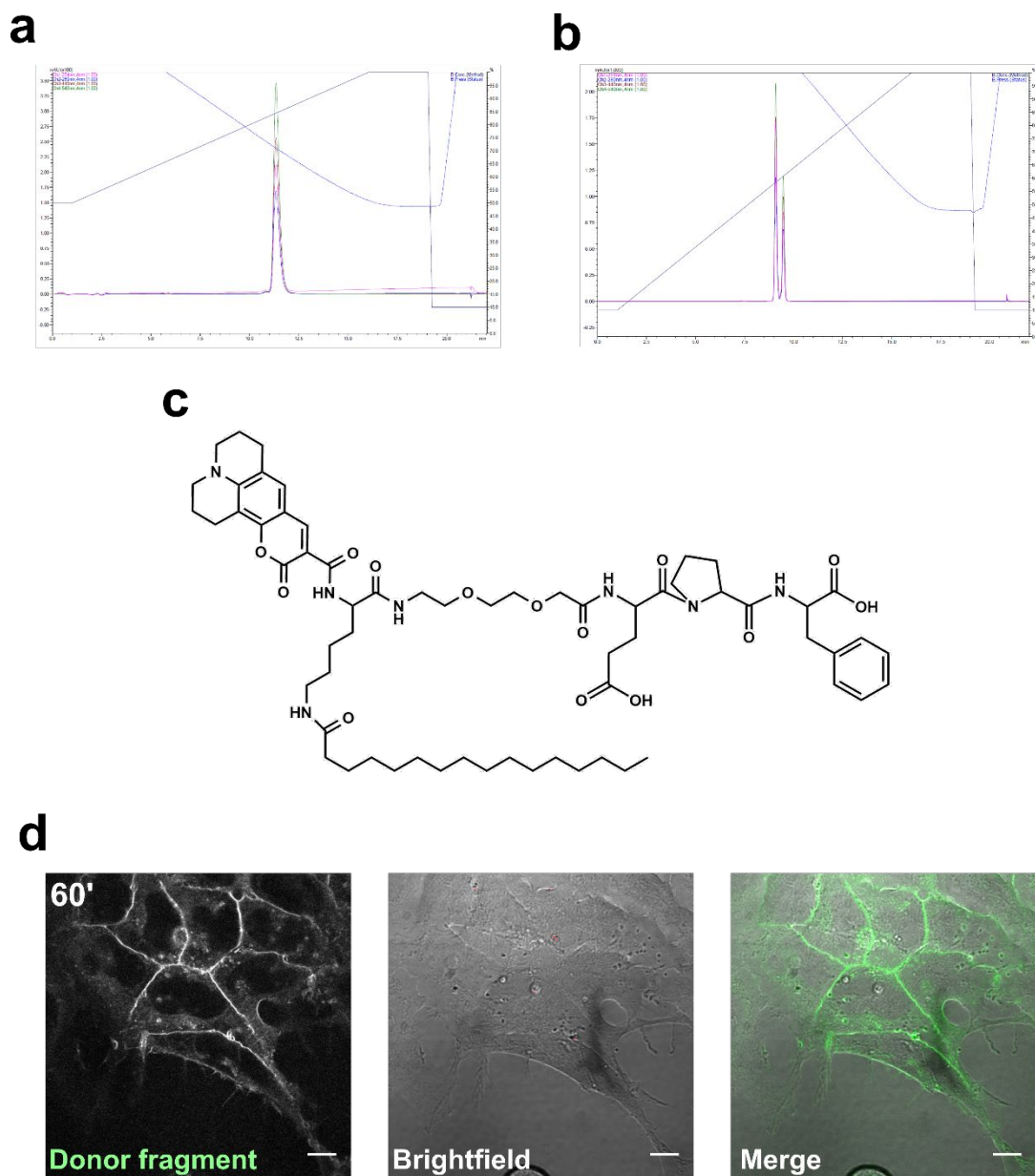


## **Supplementary Information**

### **Cathepsin G activity as a new marker for detecting airway inflammation by microscopy and flow cytometry**

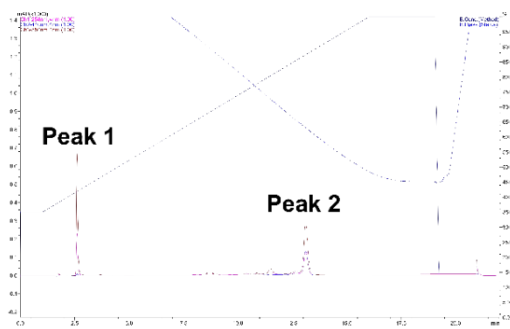
**Matteo Guerra** <sup>a,b,d</sup>, **Dario Frey** <sup>c,d</sup>, **Matthias Hagner** <sup>c,d</sup>, **Susanne Dittrich** <sup>c,d</sup>, **Michelle Paulsen** <sup>c,d</sup>, **Marcus A. Mall** <sup>c,d,e,f\*</sup>, **Carsten Schultz** <sup>a,d,g\*</sup>



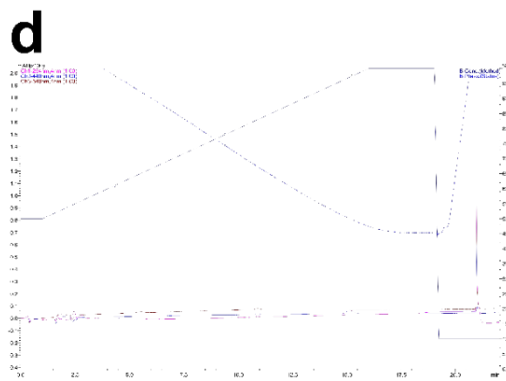
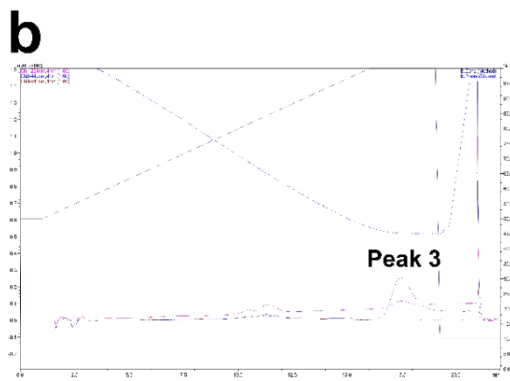
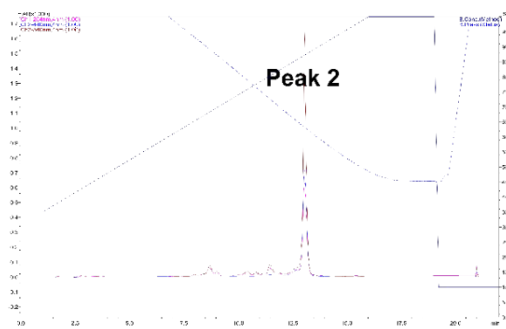
**Figure S1. Reporter purification and mSAM donor fragment localization.**

(a) Analytical HPLC of purified mSAM: gradient of 50-100% acetonitrile in water, 22 min, RT: 11.5 min. Absorbance at 450 nm (coumarin 343), 540 (TAMRA), 280 and 254 nm are shown. The single peak represents one of the two 5-(6) TAMRA isomers. (b) Analytical HPLC of purified sSAM: gradient of 10-100% acetonitrile in water, 22 min, RT: 9 and 9.5 min. Absorbance at 450 nm (coumarin 343), 540 (TAMRA), 280 and 254 nm are shown. The two peaks represent the two 5-(6) TAMRA isomers. Structure (c) and (d) plasma membrane localization of the donor fragment after 60 min incubation with HEK293 cells at 37°C. Images are representative of two independent experiments. Scale bars: 10  $\mu$ m.

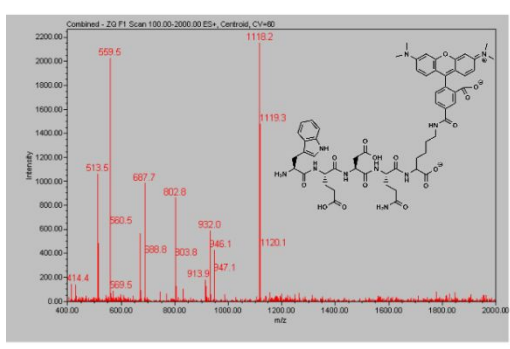
**a CG treated**



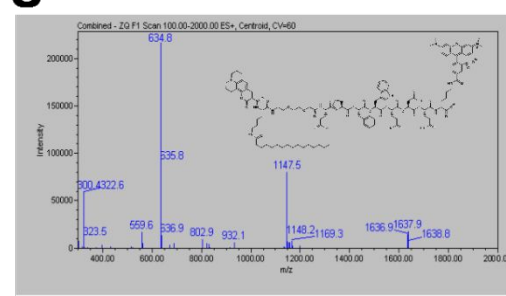
**c Untreated**



**e Peak 1**



**g Peak 2**



**f Peak 3**

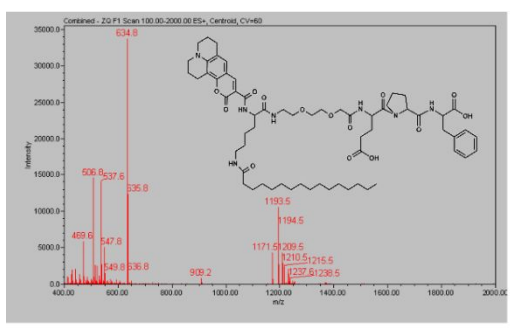


### Figure S2. mSAM cleavage site

mSAM [1mM] was resuspended in 0.1 M Tris-HCl, pH 7.5 and incubated with 200 nM human cathepsin G for 1 h at room temperature. To prove that the reporter is cleaved between Trp and Phe, the fragments originated by the enzymatic cleavage were analyzed by mass spectrometry. HPLC of CG treated (a, b) and untreated (c, d) mSAM. (a) Peak 1 in showed the characteristic TAMRA absorption and the mass corresponding to the acceptor fragment (e). The Peak 2 in (a, c) corresponded to the uncleaved reporter (coumarin 343 and TAMRA absorption and the mass shown in (g)). (b, d) Due to the impossibility to separate such a hydrophobic compound in only one HPLC run, peak 3, corresponding to the donor fragment (exclusively coumarin343 absorption and mass shown in (f)), was eluted in the subsequent runs showed in (b) and (d).

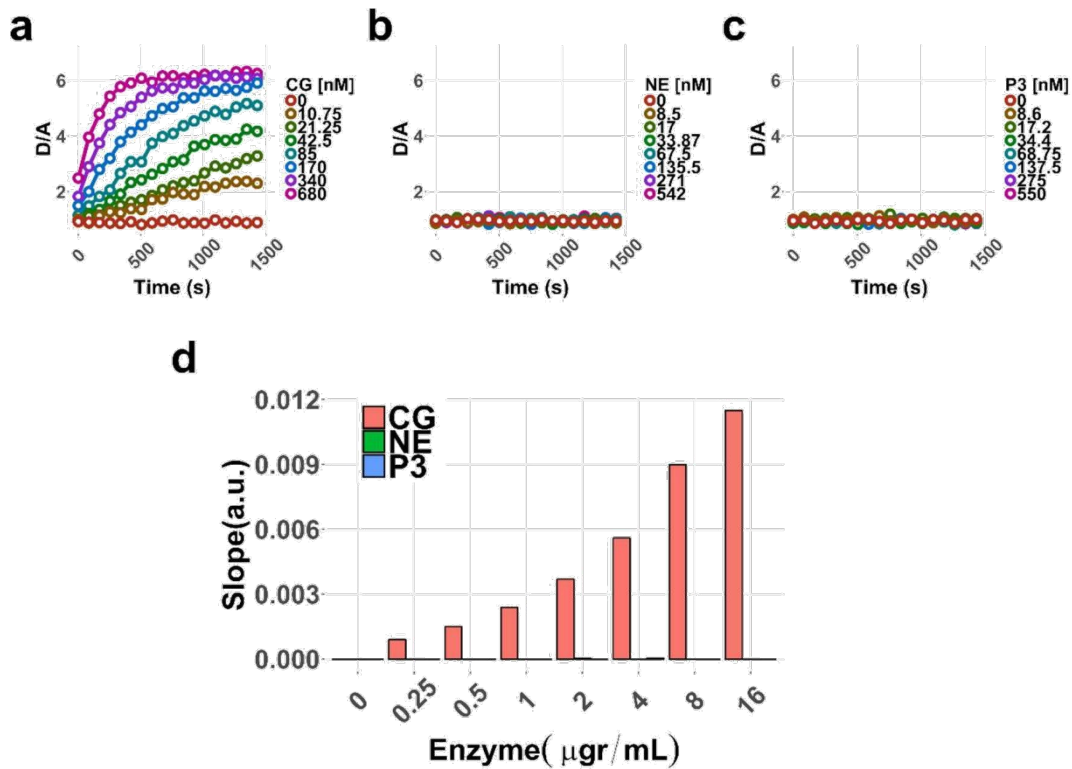


### Figure S3. sSAM sensitivity and specificity.

Fluorimetric quantification of sSAM cleavage calculated after CG (a), NE (b) and PR3 (c) addition at different molar concentrations. (d) Linear regression slopes obtained from (a), (b) and (c). Means of technical duplicates are shown.

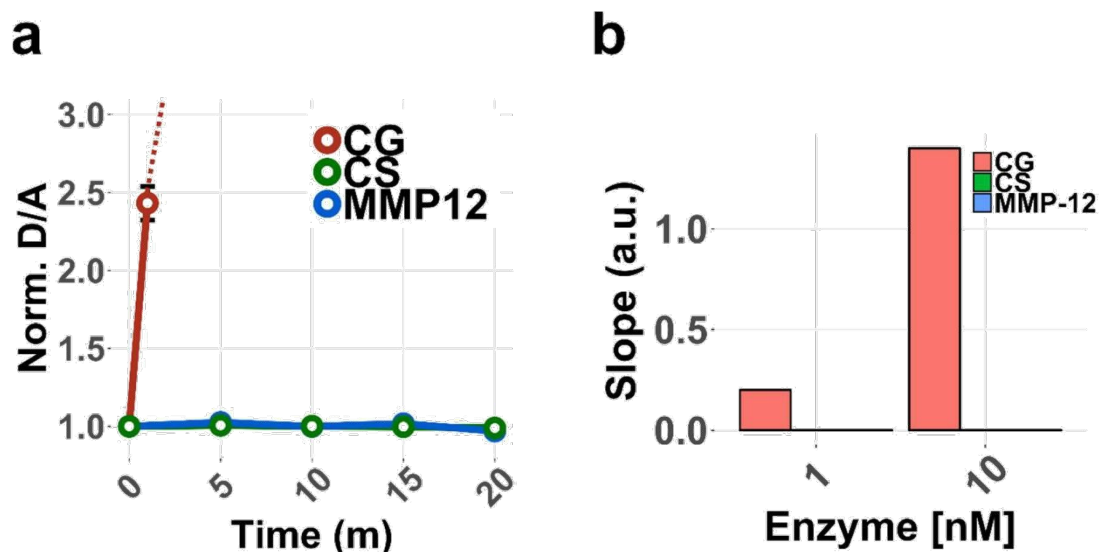


**Figure S4. mSAM specificity over matrix metalloprotease 12 (MMP12) and cathepsin S (CS).**

Fluorimetric quantification (a) and linear regression slopes (b) of mSAM cleavage rates in the presence of CG, CS, and MMP12. In (a) data are normalized to the first D/A value measured at time = 0 (in the absence of enzymes). Means  $\pm$  sem of technical triplicates are shown.

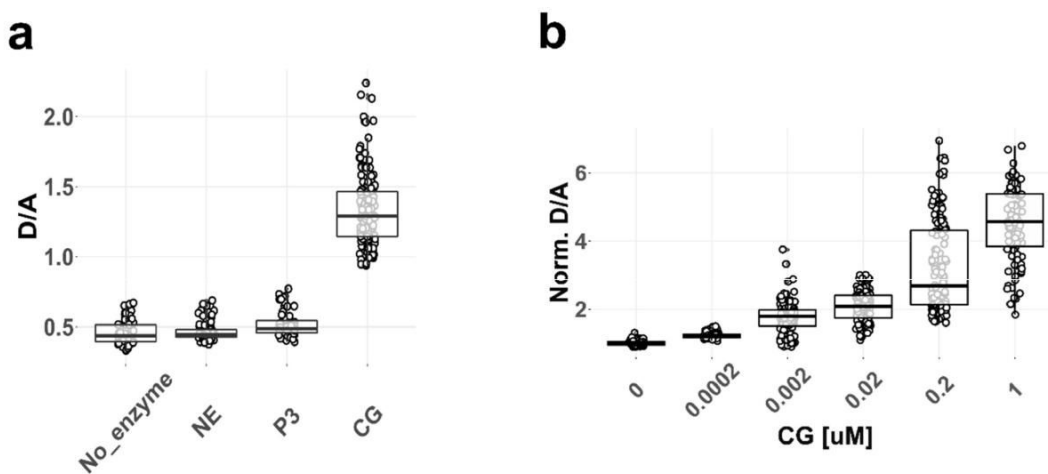


**Figure S5. mSAM characterization on HL-60 cells**

(a) Confocal microscopy quantification of donor/acceptor increase on HL-60 cells after 20 min incubation with active NE, PR3 and CG [100 nM]. (b) Dose dependent cleavage of mSAM on intact cells after 20 min incubation with different cathepsin G concentrations. N = 50-100 cells per condition, two independent replicates per experiment. In (b) donor/acceptor was normalized to the mean value calculated in the first condition (no CG addition).

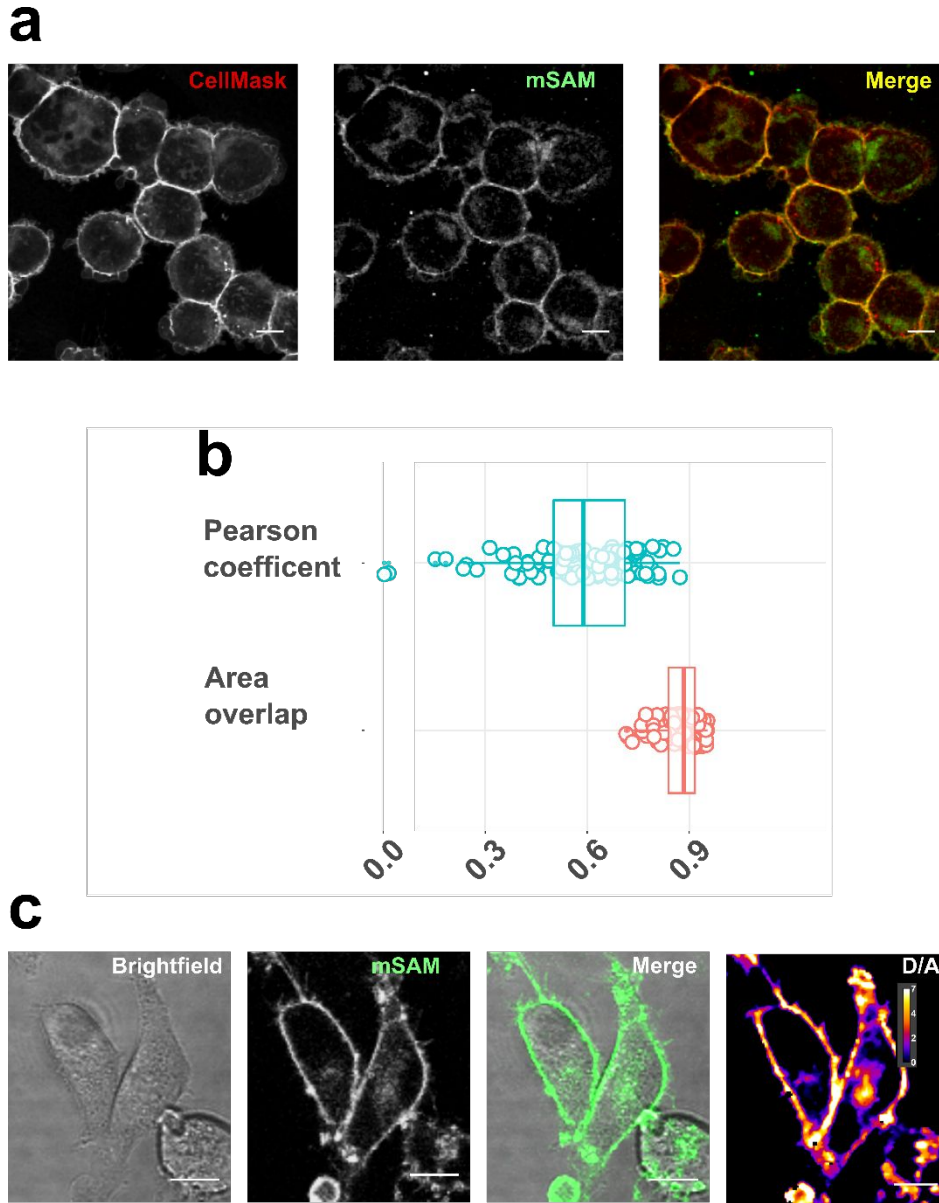


**Figure S6. Localization and cleavage of mSAM on cultured neutrophil-like (HL-60) and HEK293 cells.**

(a) Confocal microscopy of cytopinned neutrophil-like HL-60 cells incubated with the plasma membrane marker CellMask (left) and mSAM (center). Merged channels on the right. (b) Pearson coefficient and area overlap between CellMask and mSAM channels calculated for 101 cells from two independent experiments. Scale bars: 10  $\mu$ m. (c) Brightfield (left) and confocal (middle-left) microscopy of live HEK293 cells after 30 min incubation with mSAM. Merged channels (middle-right). Increase in donor/acceptor after 30 min incubation with human cathepsin G [1 nM] (right). Results are representative of three independent experiments. Scale bars: 10  $\mu$ m.

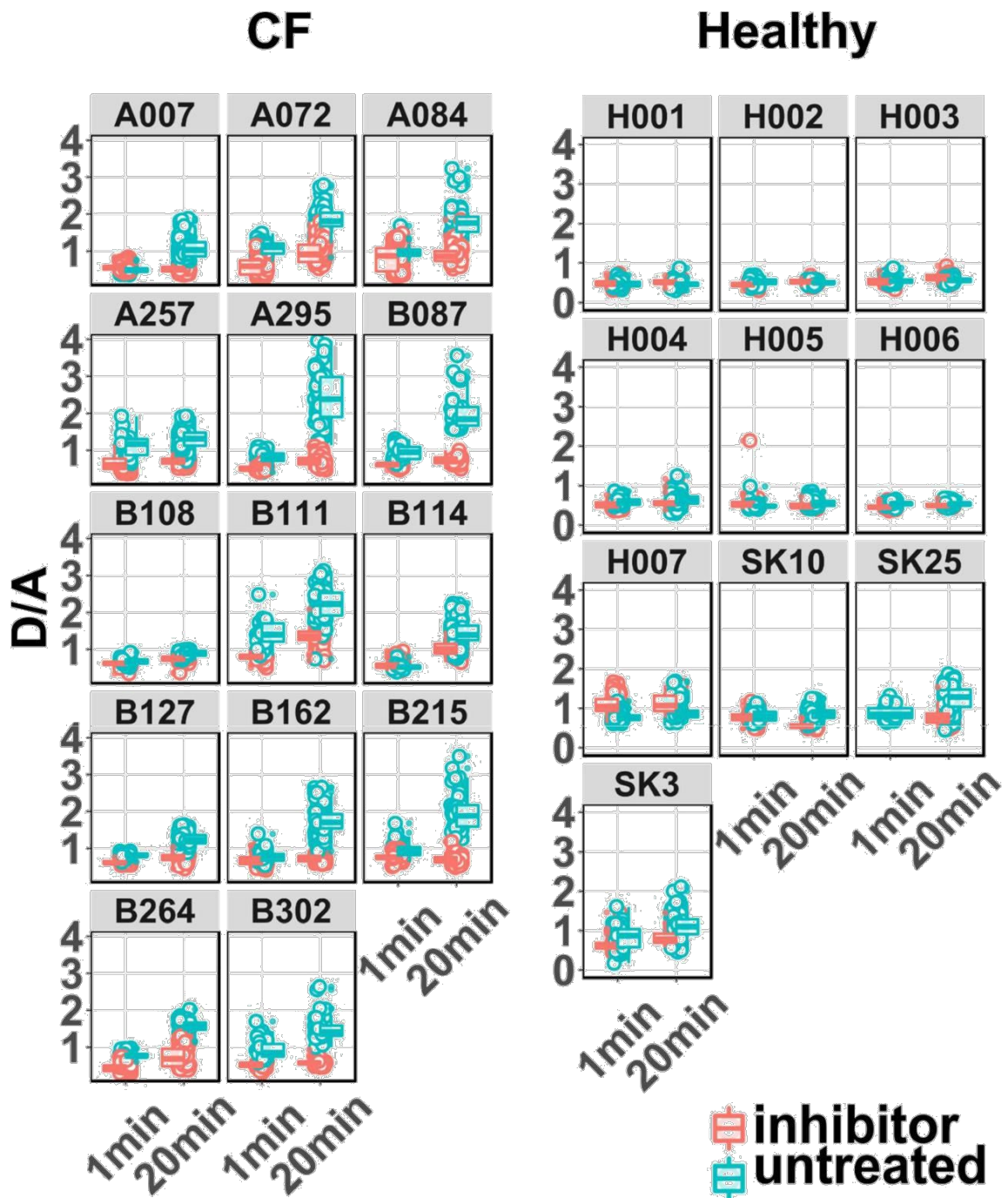


**Figure S7. Membrane-bound CG activity single patient data**

Confocal microscopy quantification of donor/acceptor emission ratio on sputum neutrophils of 14 CF patients (left) and 10 healthy donors (right). N = 50-100 cells per condition, ca. 400 cells / patient. Addition of the cOmplete™ Protease Inhibitor Cocktail served as negative control.

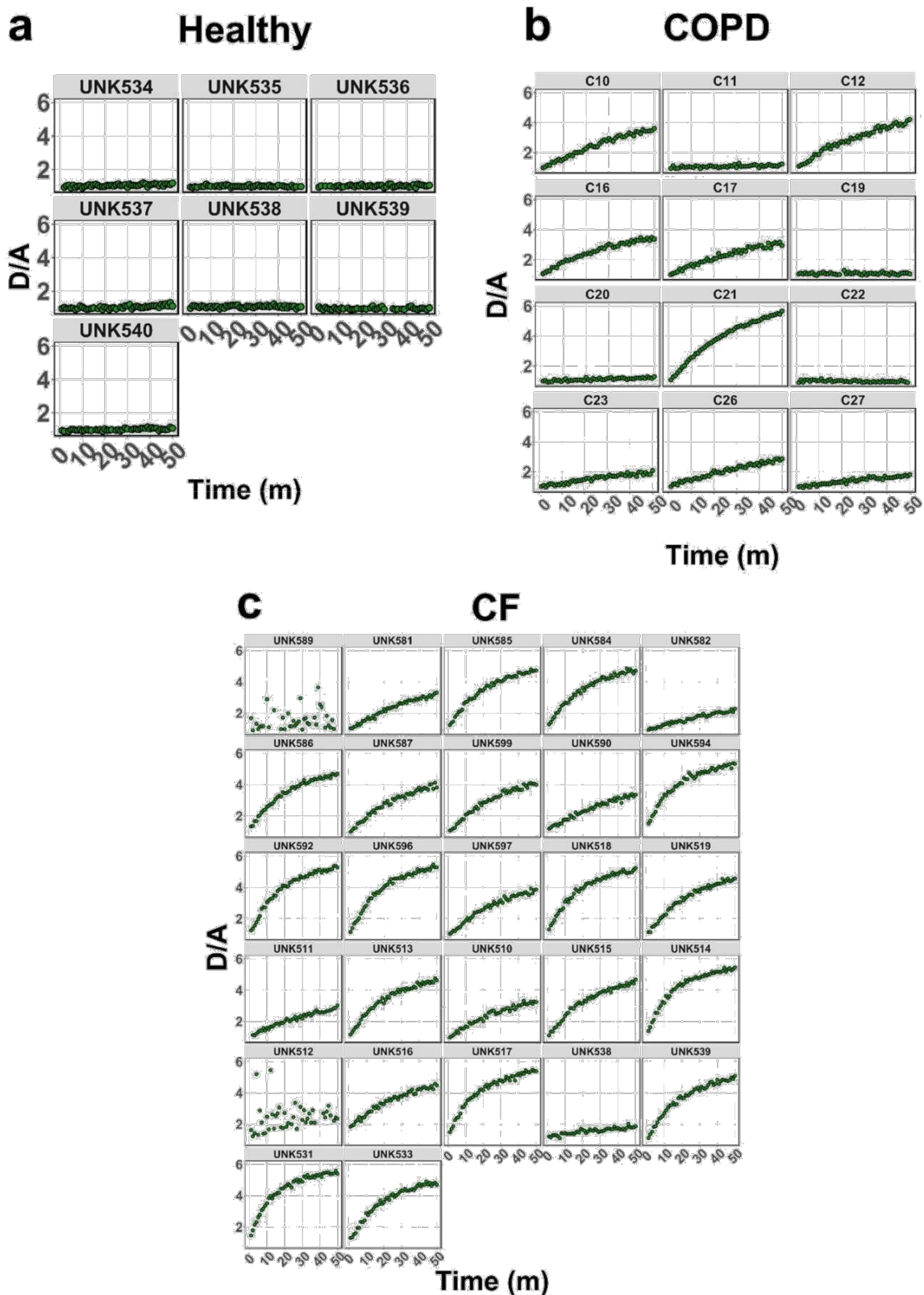


**Figure S8. Soluble CG activity single patient data**

Single traces of the time dependent quantification of donor/acceptor emission ratio in sputum supernatants of 7 healthy donors (a), 27 CF patients (b), and in 12 COPD BL fluids (c). [2 $\mu$ M] of sSAM were incubated with different dilutions of fluids. Means of technical duplicates are shown.



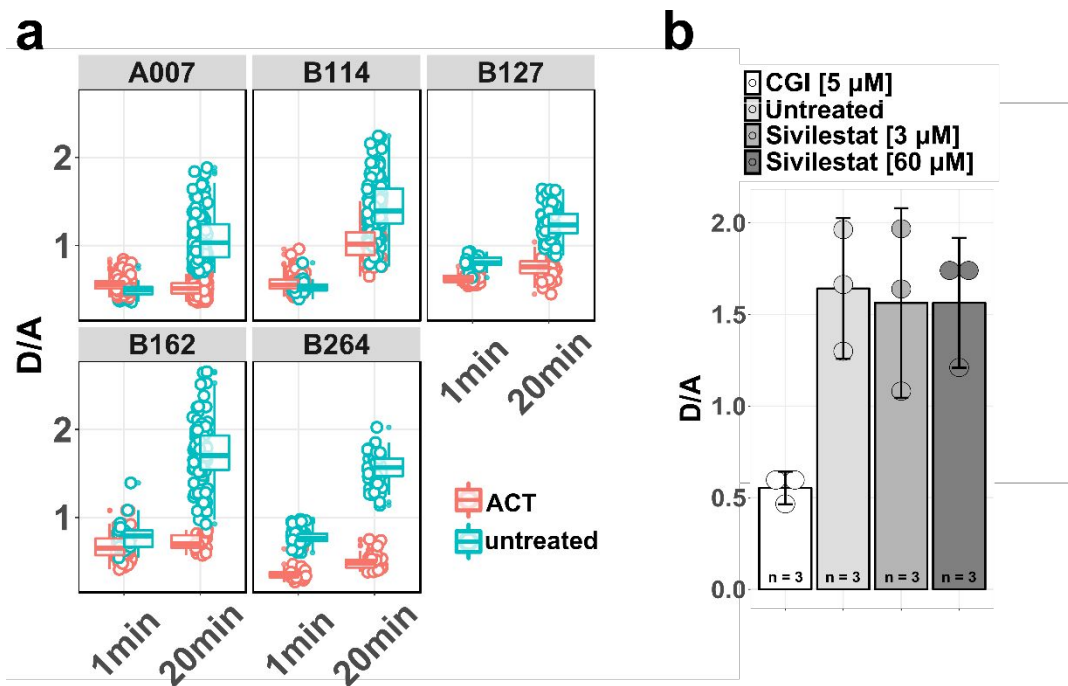


**Figure S9. *In vivo* specificity of mSAM**

(a) Single cell confocal microscopy quantification of membrane-bound CG activity on neutrophils from five CF patients in the presence of  $\alpha$ 1-antichymotrypsin [3  $\mu$ M], 1 and 20 min after mSAM addition. N = 50-100 neutrophils per condition. (b) Quantification of donor/acceptor at the surface of neutrophils derived from three CF patients, incubated for 10 min with cathepsin G inhibitor I [5  $\mu$ M], or Sivilestat [3  $\mu$ M] and [60  $\mu$ M], or left untreated. N = 50-100 neutrophils per condition. Data are derived from imaging of technical duplicates for each condition.

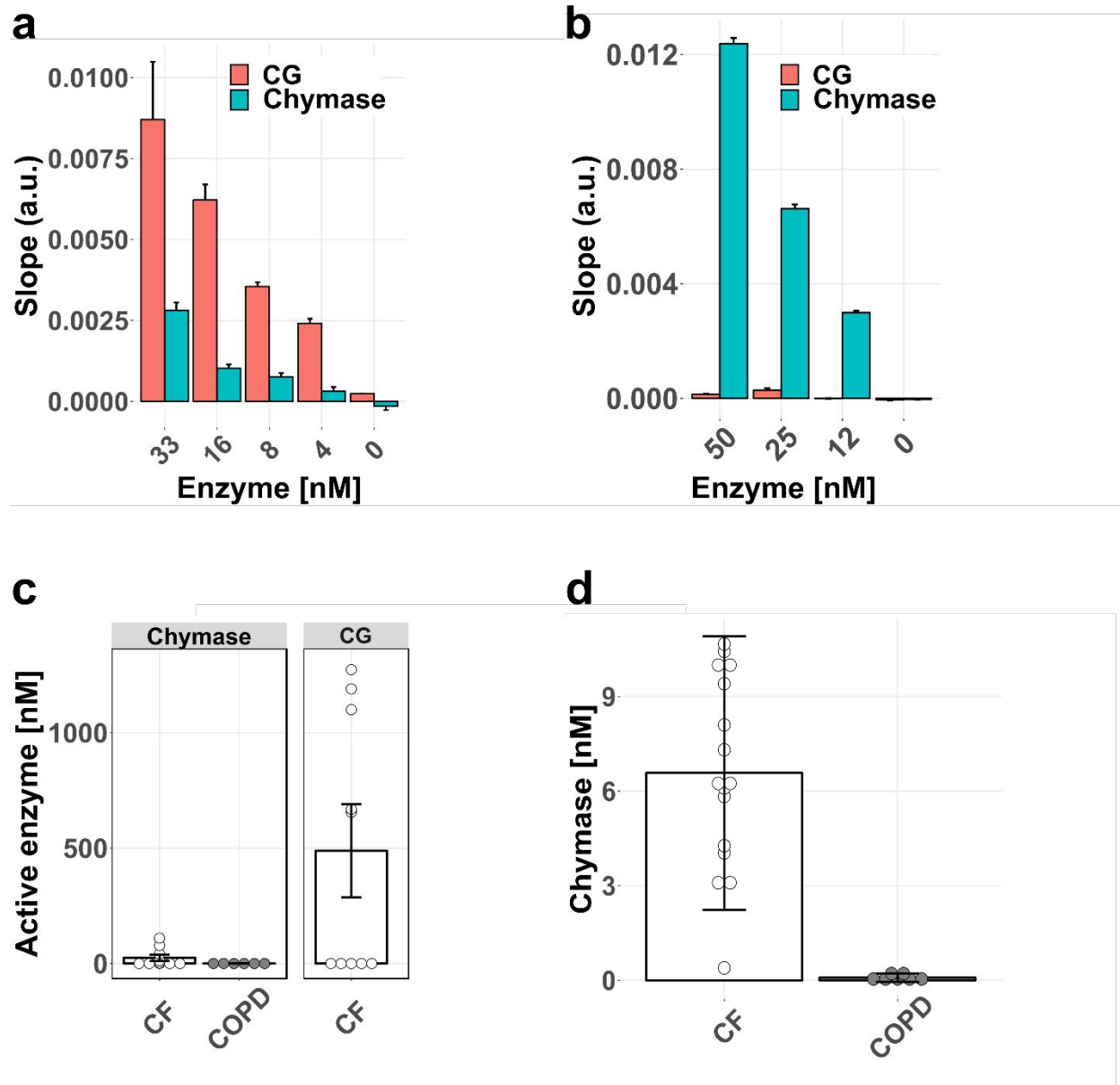


**Figure S10. Human mast cell chymase activity and concentration in CF and COPD samples**

(a) Linear regression slopes obtained from incubation of sSAM with four different concentrations of cathepsin G and human chymase. Means of technical duplicates are shown. (b) Linear regression slopes derived from incubation of the substrate Suc-AAPF-pNA with four different concentrations of cathepsin G and human chymase. Means of technical duplicates are shown. (c) (left) Quantification of active chymase in 10 CF and 6 COPD samples. Concentrations of active chymase were calculated via interpolating slopes measured in human samples with slopes obtained from standards. (right) Quantification of active cathepsin G in 10 CF sputum samples. Concentrations of active cathepsin G were calculated via interpolating slopes measured in human samples with slopes obtained from standards. Means  $\pm$  sem of technical duplicates are shown. (d) ELISA quantification of chymase concentration in sputum from patients with CF (N = 16) and BL from COPD (N = 7). Means  $\pm$  sd of technical duplicates are shown.

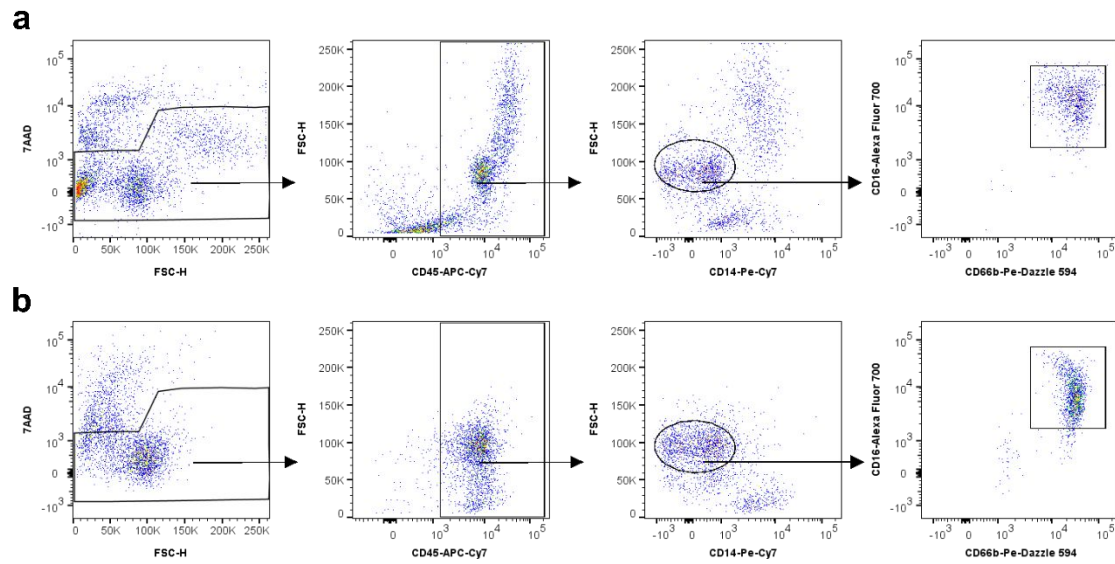


**Figure S11. Flow cytometry gating strategy**

(a, b) Representative gating strategy plots of healthy donors (a) and CF (b) sputum neutrophils. Neutrophils were gated as 7AAD<sup>-</sup>, CD45<sup>+</sup> CD66b<sup>+</sup>, CD16<sup>+</sup>, CD14<sup>-</sup> cells.

<b>CF patients table</b>		
<b>Number of subjects</b>	n	34
<b>Age (years)</b>	Median	28
	Range	16-73
<b>Sex</b>	n, males	23
	n, females	11
<b>CFTR genotype</b>		
F508del/F508del	n	18
F508del/other	n	11
other/other	n	5

**Supplementary Table 1**

<b>COPD patients table</b>		
<b>Number of subjects</b>	n	12
<b>Age (years)</b>	Median	68
	Range	50-83
<b>Sex</b>	n, males	5
	n, females	7

**Supplementary Table 2**

<b>Healthy donors table</b>		
<b>Number of subjects</b>	n	11
<b>Age (years)</b>	Median	27
	Range	23-49
<b>Sex</b>	n, males	7
	n, females	4

**Supplementary Table 3**